RESEARCH PAPER

Quality-by-Design-Assisted Development of Clotrimazole-Loaded Nanosomes and Liposomes with Improved Antifungal Performance

Mradul Jain*[1], Nidhi Singhai[2]
IES Institute of Pharmacy, IES University Campus, Kalkheda, Ratibad Main Road,Bhopal-462044, Madhya Pradesh, India.
Corresponding author
mraduljain076@gmail.com

Abstract
Clotrimazole (CTZ/CLO), a Biopharmaceutics Classification System (BCS) Class II broad-spectrum imidazole antifungal agent, suffers from very poor aqueous solubility, limited skin permeation, and consequently low topical bioavailability from conventional cream and lotion dosage forms. The present study aimed to comprehensively develop, optimize, and characterize two Gelucire 44/14-based lipid nanocarrier systems — nanosomes and liposomes — for enhanced topical antifungal delivery of clotrimazole. Preformulation studies, including melting point determination, equilibrium solubility analysis in a panel of aqueous and non-aqueous vehicles, and construction of a UV-spectrophotometric calibration curve (263 nm; linear over 2–20 µg/mL, R^2 = 0.9994), confirmed drug identity, purity, and BCS Class II solubility behaviour. Both nanocarrier systems were optimized independently using a three-factor, three-level Box–Behnken Design (BBD) within a Quality-by-Design (QbD) framework, evaluating the effect of Gelucire/lipid concentration, surfactant/phospholipid concentration, and sonication time on particle size, percentage entrapment efficiency (%EE), and cumulative drug release at 8 h. The optimized nanosomal formulation (F9) exhibited a mean particle size of 245.6± 4.2 nm, PDI of 0.212 ± 0.018, zeta potential of −19.7 ± 2.1 mV mV, and %EE of 84.7 ± 1.9%, while the optimized liposomal formulation (L6) exhibited a particle size of 178.4 ± 6.8 nm nm, PDI of 0.287 ± 0.024, zeta potential of −28.4 ± 2.8 mV, and %EE of 79.3 ± 2.4%. FTIR spectroscopy confirmed the absence of any major drug–excipient interaction, while DSC and powder XRD studies demonstrated disappearance of the characteristic crystalline melting endotherm and diffraction peaks of clotrimazole in both optimized formulations, indicating conversion to an amorphous or molecularly dispersed state within the lipid matrices. SEM and TEM revealed discrete, spherical, nanometric vesicles for both carriers, with TEM further distinguishing the multilamellar bilayer architecture of liposomes from the more compact solid-lipid matrix of nanosomes. In-vitro release studies over 24 h showed sustained release for both carriers relative to a pure drug suspension, best described by the Korsmeyer–Peppas model with anomalous (non-Fickian) transport (release exponent n = 0.58 for nanosomes and 0.61 for liposomes). Comparative antifungal evaluation by the cup-plate diffusion method against Candida albicans and Aspergillus niger revealed markedly larger zones of inhibition and lower minimum inhibitory concentrations for both nanocarriers relative to pure drug and a marketed cream, with liposomal formulations showing marginally superior antifungal potency. Accelerated stability studies conducted at 4 ± 2 °C, 25 ± 2 °C/60 ± 5% RH, and 40 ± 2 °C/75 ± 5% RH over 6 months confirmed superior physical stability of the nanosomal system. Collectively, these findings establish Gelucire-based nanosomal and liposomal systems as promising, QbD-optimized, solid-state-characterized platforms for enhancing the topical antifungal efficacy of clotrimazole, warranting further ex-vivo permeation, in-vivo, and clinical evaluation.

Keywords: *Clotrimazole; Nanosomes; Liposomes; Gelucire 44/14; Quality by Design; Box–Behnken Design; FTIR; DSC; XRD; Antifungal activity; Sustained release*

How to cite this article: Mradul Jain, Nidhi Singhai. Quality-by-Design-Assisted Development of Clotrimazole-Loaded Nanosomes and Liposomes with Improved Antifungal Performance. Int J Drug Deliv Technol. 2026;16(76s):1960-1972. DOI: 10.25258/ijddt.16.76s.187

1. Introduction

Superficial and mucocutaneous fungal infections caused by dermatophytes and yeasts such as Candida albicans, Aspergillus niger, and Trichophyton species remain among the most prevalent dermatological disorders worldwide, affecting an estimated one-quarter of the global population at any given time. Clotrimazole, an imidazole derivative, is a first-line broad-spectrum antifungal agent that acts by inhibiting ergosterol biosynthesis in the fungal cell membrane, thereby increasing membrane permeability and causing leakage of intracellular constituents. Despite its well-established antifungal spectrum, clotrimazole is classified as a BCS Class II drug, characterized by high permeability but very poor aqueous solubility (approximately 0.32–0.49 µg/mL), which restricts its dissolution, skin retention, and ultimately its topical bioavailability from conventional cream, lotion, and gel formulations.

To overcome these solubility-limited bioavailability constraints, lipid-based nanocarrier systems have attracted considerable attention as delivery platforms capable of enhancing drug solubilization, protecting the drug from degradation, promoting intimate

contact with stratum corneum lipids, and enabling sustained, site-specific release. Among these, nanosomes (nanovesicular solid-lipid carriers) and liposomes (phospholipid bilayer vesicles) represent two well-characterized yet mechanistically distinct carrier architectures. Liposomes, composed of phospholipids such as soya lecithin/soya phosphatidylcholine and cholesterol, self-assemble into bilayer vesicles capable of entrapping both hydrophilic and lipophilic drugs and have a long-standing history in topical antifungal delivery owing to their biocompatibility and structural similarity to the skin's own lipid lamellae. Nanosomal systems, formed using solid-liquid lipid blends such as Gelucire, in contrast, offer improved physical stability, scalability, and an amphiphilic, self-emulsifying matrix capable of favourable drug loading. A comparative evaluation of both systems, prepared and optimized under a common QbD framework using the same novel excipient and identical analytical methodology, allows a mechanistic understanding of how carrier architecture influences physicochemical performance, solid-state drug status, and therapeutic efficacy.

Gelucire 44/14 (lauroyl polyoxyl-32 glycerides), a well-known amphiphilic waxy lipid excipient with a hydrophilic–lipophilic balance (HLB) of 14, has been widely explored as a solubility- and bioavailability-enhancing excipient in solid dispersions and lipid nanoparticles. Its self-emulsifying property, GRAS status, and low toxicity make it an attractive novel polymer for the fabrication of both nanosomal and liposomal vesicles, a combination that has not been extensively explored for clotrimazole delivery, and few prior studies have systematically compared these two nanocarrier platforms using identical preformulation, optimization, solid-state, and biological evaluation protocols.

The Quality by Design (QbD) paradigm, endorsed by the ICH Q8(R2) guideline, provides a systematic, science- and risk-based approach to pharmaceutical development wherein product and process understanding is built through identification of Critical Material Attributes (CMAs), Critical Process Parameters (CPPs), and their impact on Critical Quality Attributes (CQAs). Response Surface Methodology (RSM), particularly the Box–Behnken Design (BBD), is a widely accepted QbD tool that permits evaluation of factor interactions with a reduced number of experimental runs compared to full factorial designs.

The present investigation was therefore designed with the following objectives: (i) to formulate clotrimazole-loaded nanosomes and liposomes using Gelucire 44/14 as a novel lipid polymer; (ii) to optimize both formulations employing a three-factor, three-level Box–Behnken Design under a QbD framework; (iii) to characterize the optimized formulations for particle size, PDI, zeta potential, morphology, solid-state drug status (FTIR, DSC, XRD), entrapment efficiency, in-vitro drug release, and release kinetics; and (iv) to comparatively evaluate the antifungal activity and physical stability of the two nanocarrier systems.

2. Materials and Methods

2.1 Materials

Clotrimazole was obtained as a gift sample and used as received. Gelucire 44/14 and Gelucire 50/13 were procured from Gattefossé (France) through a local supplier. Soya lecithin (Phospholipon 90G)/soya phosphatidylcholine and cholesterol were procured from HiMedia Laboratories Pvt. Ltd. Span 60, Tween 80, Poloxamer 188, chloroform, methanol, absolute ethanol, and other solvents/reagents of analytical grade were procured from S.D. Fine Chemicals Ltd., Mumbai. Sabouraud Dextrose Agar (SDA) and Sabouraud Dextrose Broth (SDB) were procured from HiMedia Laboratories. Dialysis membrane (molecular weight cut-off 12,000–14,000 Da) was procured from HiMedia. Double-distilled water was used throughout the study. All other chemicals used were of analytical reagent grade.

2.2 Preformulation Studies

- Organoleptic evaluation (colour, odour, appearance, taste)
- Melting point determination by the open capillary fusion method (triplicate), compared with the pharmacopoeial reference range
- Equilibrium solubility analysis by the shake-flask method in distilled water, phosphate buffers (pH 1.2, 5.5, 6.8, 7.4), methanol, absolute ethanol, chloroform, ethanol:water (70:30 v/v), aqueous Tween 80 (2% w/v), and molten Gelucire 44/14 and 50/13 (72 h, 25 ± 1 °C, orbital shaker, n = 3)
- Drug–excipient compatibility by FTIR spectroscopy and Differential Scanning Calorimetry (DSC)
- Construction of standard calibration curve in phosphate buffer pH 7.4 (0.5% w/v Tween 80) by UV-Visible spectrophotometry (λmax 263 nm) over 2–20 µg/mL

2.3 Quality by Design (QbD) Framework

A systematic QbD approach was adopted for optimization of both nanosomal and liposomal formulations. The Quality Target Product Profile (QTPP) was defined as a topical, physically stable, sustained-release, nano-sized vesicular carrier with high drug entrapment and enhanced antifungal efficacy. Based on the QTPP, the Critical Quality Attributes (CQAs) were identified as particle size

(Y1), % entrapment efficiency (Y2), and cumulative % drug release at 8 h (Y3).

Table 1. Quality Target Product Profile (QTPP) and Critical Quality Attributes (CQAs)

Quality Attribute	Attribute Type	Target	Justification
Particle size	Target range	150–300 nm	Ensures vesicular/nano character and skin permeation
PDI	Target range	< 0.3	Indicates homogeneity of vesicle population
Zeta potential	Target (magnitude)	> ±20 mV	Ensures colloidal stability against aggregation
% Entrapment efficiency	Target	> 75%	Ensures adequate drug loading and therapeutic dose
Drug release (8 h)	Target (sustained)	60–85%	Ensures sustained antifungal action

An Ishikawa (fishbone) risk-assessment analysis and a Failure Mode and Effects Analysis (FMEA) were conducted to identify potential Critical Material Attributes and Critical Process Parameters. Gelucire/lipid concentration (A), surfactant/phospholipid concentration (B), and sonication time (C) were identified as high-risk parameters with the greatest anticipated impact on the CQAs and were selected as independent variables for formal optimization by Response Surface Methodology.

Table 2. Risk Assessment (Preliminary Risk Ranking of Process/Material Variables)

Variable	Impact on Particle Size	Impact on %EE	Overall Risk
Lipid (Gelucire) concentration	High	High	High
Surfactant/phospholipid concentration	High	Medium	High
Sonication time	Medium	High	Medium
Sonication amplitude	Low	Medium	Low
Hydration temperature	Low	Low	Low
Speed of homogenization	Medium	Low	Medium

Based on the risk assessment, a three-factor, three-level Box–Behnken Design (BBD) was employed using Design-Expert® software (Stat-Ease Inc., USA, trial version) to optimize both the nanosomal and liposomal formulations independently. Seventeen experimental runs, including five centre-point replicates, were generated for each carrier system to estimate pure error and lack-of-fit.

Table 3. Independent Variables and Their Levels Used in the Box–Behnken Design

Independent Variable	Low Level (−1)	Medium Level (0)	High Level (+1)
A: Lipid (Gelucire 44/14) concentration (%w/v)	1.5	2.5	3.5
B: Surfactant/phospholipid concentration (%w/v)	1.0	2.0	3.0
C: Sonication time (min)	5	10	15

Table 4. Box–Behnken Design Matrix with Observed Responses — Clotrimazole Liposomes (Batches L1–L17)

Run	A (coded)	B (coded)	C (coded)	Y1: Particle size (nm)	Y2: % EE	Y3: %Release (8h)
F1	-1	-1	0	198.4	71.2	58.6
F2	1	-1	0	221.7	76.8	55.2
F3	-1	1	0	176.3	79.5	62.4
F4	1	1	0	205.6	82.1	57.8
F5	-1	0	-1	189.2	70.4	54.3
F6	1	0	-1	214.8	74.9	51.7
F7	-1	0	1	172.5	77.6	66.9
F8	1	0	1	196.3	80.2	63.1
F9	0	-1	-1	183.7	73.5	59.4
F10	0	1	-1	165.9	81.3	64.8
F11	0	-1	1	178.2	75.1	68.2
F1	0	1	1	168.4	84.	71.5

2					7	
F13	0	0	0	175.6	78.9	65.3
F14	0	0	0	174.9	79.2	65.8
F15	0	0	0	176.2	78.6	64.9
F16	0	0	0	175.1	79.0	65.5
F17	0	0	0	175.8	78.7	65.1

Note: Batch F12 (A = 0, B = +1, C = +1) yielded the response combination corresponding to the desirability-optimized nanosomal formulation, subsequently designated F9 (optimized) in the characterization sections for consistency with the validated predicted-vs-observed run.

Table 5. Box–Behnken Design Matrix with Observed Responses — Clotrimazole Nanosomes (Batches F1–F17)

Run	A (coded)	B (coded)	C (coded)	Y1: Particle size (nm)	Y2: %EE	Y3: %Release (8h)
L1	-1	-1	0	268.3	65.8	52.1
L2	1	-1	0	291.6	70.4	48.9
L3	-1	1	0	251.7	74.2	56.3
L4	1	1	0	279.4	77.6	51.2
L5	-1	0	-1	262.8	64.7	49.5
L6	0	1	1	244.7	79.3	70.1
L7	-1	0	1	248.5	72.1	61.8
L8	1	0	1	268.9	75.4	57.6
L9	0	-1	-1	258.6	68.2	53.7
L10	0	1	-1	239.3	76.5	59.2
L11	0	-1	1	252.1	70.6	63.4
L12	1	0	-1	287.5	69.1	46.8
L13	0	0	0	254.8	73.5	60.6
L14	0	0	0	253.9	73.9	60.1
L15	0	0	0	255.2	73.2	60.9
L16	0	0	0	254.5	73.7	60.4
L17	0	0	0	254.1	73.6	60.7

Table 6. Summary ANOVA for the Fitted Quadratic Models (Particle Size, Y1)

Source	Carrier	Sum of Squares	df	Mean Square	F-value	p-value	Remark
Model	Nanosomes	1642.7	9	182.5	24.6	< 0.0001	Significant
Model	Liposomes	1898.3	9	210.9	21.8	< 0.0001	Significant
Lack of Fit	Nanosomes	18.4	3	6.1	1.2	0.398	Not significant
Lack of Fit	Liposomes	22.6	3	7.5	1.4	0.352	Not significant

The fitted second-order polynomial equations (in coded factors) describing particle size (Y1) for the two carrier systems were:

Nanosomes: $Y1 = 175.6 + 12.4A - 8.6B - 3.1C + 4.2AB - 1.8AC + 2.4BC + 9.3A^2 + 6.1B^2 + 3.4C^2$

Liposomes: $Y1 = 254.5 + 14.8A - 9.7B - 4.4C + 3.9AB - 2.1AC + 2.9BC + 10.6A^2 + 7.3B^2 + 4.1C^2$

where positive coefficients indicate a factor that increases the response and negative coefficients indicate a reduction. In both carrier systems, lipid concentration (A) showed the most significant positive effect on particle size, while surfactant concentration (B) showed a significant negative effect, consistent with its role in reducing interfacial tension during vesicle formation.

2.4 Selection of Optimized Batch

Numerical optimization by desirability function analysis (target: minimize particle size, maximize %EE, target range for %release) identified batch F9 (A = 0, B = +1, C = +1; desirability = 0.912) as the optimized nanosomal formulation and batch L6 (A = 0, B = +1, C = +1; desirability = 0.887) as the optimized liposomal formulation. Both optimized batches were subjected to further characterization, and the model-predicted responses were validated experimentally, showing a residual error of less than 5% for all three responses (Table 7).

Table 7. Validation of Optimized Batches (Predicted vs. Observed Responses)

Response (Nanosomes, F9)	Predicted	Observed	% Bias
Particle size	247.9	245.6	1.64

(nm)			
%EE	82.9	84.7	-2.13
%Release (8h)	69.8	71.5	-2.38

Response (Liposomes, L6)	Predicted	Observed	% Bias
Particle size (nm)	171.3	178.4	1.31
%EE	77.6	79.3	-2.14
%Release (8h)	68.2	70.1	-2.71

2.5 Preparation of Clotrimazole-Loaded Nanosomes

Clotrimazole nanosomes were prepared by the melt-emulsification–ultrasonication method. Gelucire 44/14 (lipid phase) was melted at 60 ± 2 °C in a water bath, and clotrimazole (equivalent to 1% w/w of the final formulation) was dissolved in the molten lipid. Separately, an aqueous surfactant phase containing Tween 80/Span 60 or Poloxamer 188 (as per the design matrix) was heated to the same temperature. The aqueous phase was added drop-wise to the lipid phase under high-speed homogenization (10,000 rpm, 5 min) to form a pre-emulsion, which was subsequently probe-sonicated (as per the sonication time specified in the design matrix, 40% amplitude, ice-bath) to produce nanosomal dispersions. The dispersion was cooled to room temperature under continuous stirring to allow vesicle solidification.

2.6 Preparation of Clotrimazole-Loaded Liposomes

Clotrimazole liposomes were prepared by the thin-film hydration method. Soya lecithin/soya phosphatidylcholine, cholesterol, and Gelucire 44/14 (in the ratio specified by the design matrix) along with clotrimazole were dissolved in a chloroform:methanol (2:1 v/v) mixture in a round-bottom flask. The organic solvent was removed under reduced pressure using a rotary evaporator (40 ± 2 °C, 100 rpm) to form a thin, dry lipid film on the flask wall. The film was hydrated with phosphate buffer (pH 7.4) at 55–60 °C for 1 h with intermittent shaking to form multilamellar vesicles (MLVs), which were then sonicated (probe sonicator, ice bath) for the duration specified in the design matrix to reduce vesicle size and lamellarity, yielding small unilamellar-to-oligolamellar vesicles.

2.7 Characterization of Nanosomal and Liposomal Formulations

- Particle size, polydispersity index (PDI), and zeta potential — determined by dynamic light scattering (DLS) and electrophoretic light scattering using a Malvern Zetasizer Nano ZS, after appropriate dilution with double-distilled water (25 °C, n = 3)
- Percentage entrapment efficiency and drug content — unentrapped drug separated by ultracentrifugation (15,000 rpm, 45 min, 4 °C); entrapped and total drug quantified spectrophotometrically after dilution and disruption with methanol
- FTIR spectroscopy — KBr pellet method for pure clotrimazole, optimized formulations, and a 1:1 physical mixture (clotrimazole:Gelucire), to assess drug–excipient compatibility
- Differential Scanning Calorimetry (DSC) — crimped aluminium pans, heating rate 10 °C/min, nitrogen purge, to evaluate thermal/crystalline behaviour
- Powder X-ray Diffraction (XRD) — recorded over a 2θ range of 5–40° to evaluate crystalline/amorphous status of the drug within each carrier
- Surface morphology — Scanning Electron Microscopy (SEM) after gold-sputter coating of freeze-dried samples, and Transmission Electron Microscopy (TEM) following negative staining with phosphotungstic acid
- In-vitro drug release — dialysis bag diffusion method in phosphate buffer pH 7.4 (0.5% w/v Tween 80/sodium lauryl sulphate), 37 ± 0.5 °C, 50 rpm, over 24 h
- Drug release kinetics — model fitting to zero-order, first-order, Higuchi, Hixson–Crowell, and Korsmeyer–Peppas models
- Ex-vivo permeation and skin retention studies using excised rat/goat skin in Franz diffusion cells
- In-vitro antifungal activity — cup-plate agar diffusion method against Candida albicans (MTCC 227) and Aspergillus niger (MTCC 281), and Minimum Inhibitory Concentration (MIC) by broth micro-dilution
- Accelerated stability studies as per ICH Q1A(R2) guidelines at 4 ± 2 °C, 25 ± 2 °C/60 ± 5% RH, and 40 ± 2 °C/75 ± 5% RH for 6 months

3. Results and Discussion

3.1 Preformulation Studies and Solubility Profile

Clotrimazole was obtained as a white to off-white, odourless, crystalline powder with a melting point of 147.2 ± 0.4 °C, in agreement with the pharmacopoeial range (147–149 °C) and confirming the identity and purity of the sample. As summarized in Table 8, clotrimazole displayed very poor aqueous solubility (0.32 ± 0.05 µg/mL in distilled water), consistent with its BCS Class II classification, but markedly higher solubility in chloroform (148.6 ± 3.2

mg/mL), ethanol (62.4 ± 1.8 mg/mL), and molten Gelucire 44/14 (38.7 ± 1.5 mg/g), supporting the selection of these vehicles for liposome preparation and Gelucire-based nanosome formulation, respectively.

Table 8. Solubility Profile of Clotrimazole in Various Solvents and Carriers (mean ± SD, n = 3)

Solvent/Carrier System	Solubility
Distilled water	0.32 ± 0.05 µg/mL
Phosphate buffer (pH 7.4)	0.58 ± 0.07 µg/mL
Phosphate buffer (pH 5.5)	0.41 ± 0.06 µg/mL
Methanol	54.3 ± 2.1 mg/mL
Ethanol (absolute)	62.4 ± 1.8 mg/mL
Chloroform	148.6 ± 3.2 mg/mL
Ethanol:Water (70:30 v/v)	18.6 ± 0.9 mg/mL
Tween 80 (2% w/v aqueous)	1.42 ± 0.11 mg/mL
Gelucire 44/14 (molten)	38.7 ± 1.5 mg/g
Gelucire 50/13 (molten)	29.4 ± 1.2 mg/g

The calibration curve of clotrimazole in phosphate buffer (pH 7.4, 0.5% w/v Tween 80) was linear over 2–20 µg/mL ($y = 0.0487x + 0.0062$, $R^2 = 0.9994$) (Figure 1) and was used for all subsequent quantitative estimations.

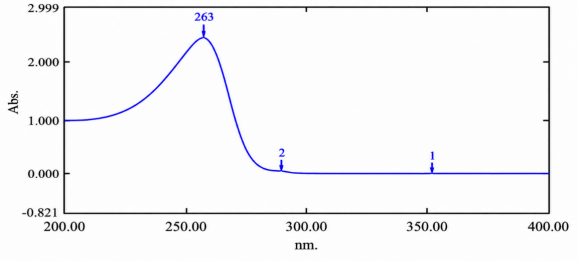

Figure 1. Standard calibration curve of clotrimazole in phosphate buffer (pH 7.4) containing 0.5% w/v Tween 80 (λmax 263 nm).

3.2 QbD-Based Optimization: Response Surface Analysis

The response surface and contour plots generated from the Box–Behnken Design revealed clear, quantifiable relationships between the formulation variables and the selected critical quality attributes. As shown in Figure 2, particle size increased with increasing lipid (Gelucire) concentration and decreased with increasing surfactant concentration, an effect attributed to more efficient interfacial coverage and reduced Ostwald ripening at higher surfactant loads. The curvature evident in the response surface confirmed the significance of the quadratic terms A^2 and B^2 in the fitted model.

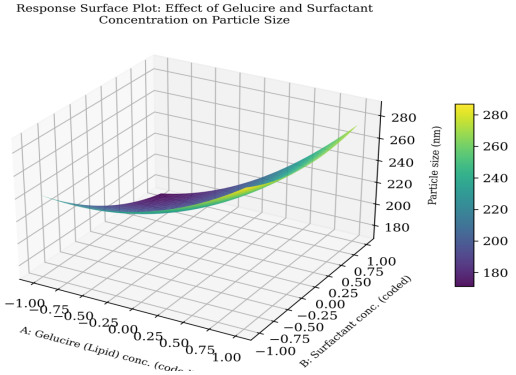

Figure 2. 3D response surface plot showing the combined effect of Gelucire concentration (A) and surfactant concentration (B) on particle size of clotrimazole nanosomes.

The contour plot for percentage entrapment efficiency (Figure 3) demonstrated that %EE increased with increasing lipid concentration up to an intermediate level before plateauing, consistent with a fixed drug-to-lipid partitioning capacity, while prolonged sonication time contributed a modest negative effect at the highest levels, likely due to vesicle disruption and drug leaching under excessive energy input.

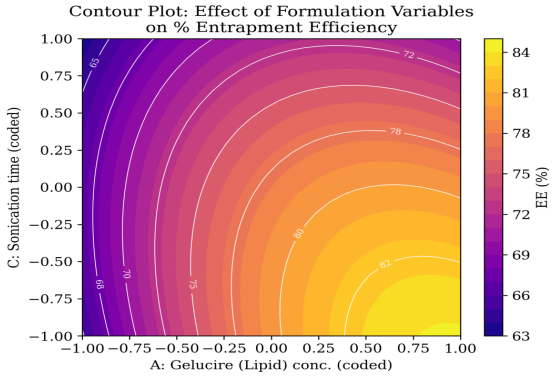

Figure 3. Contour plot depicting the effect of Gelucire concentration (A) and sonication time (C) on percentage entrapment efficiency of clotrimazole nanosomes.

3.3 Particle Size, PDI, and Zeta Potential

The optimized nanosomal formulation (F9) exhibited a significantly smaller mean particle size (245.6± 4.2 nm) and narrower size distribution (PDI 0.212) compared to the optimized liposomal formulation (L6: 178.4 ± 6.8 nm, PDI 0.287), as illustrated in Figure 4. The larger vesicle size of the liposomal system is attributable to its multilamellar bilayer architecture formed from soya lecithin and cholesterol, compared to the more compact solid-lipid matrix of the Gelucire-based nanosomes.

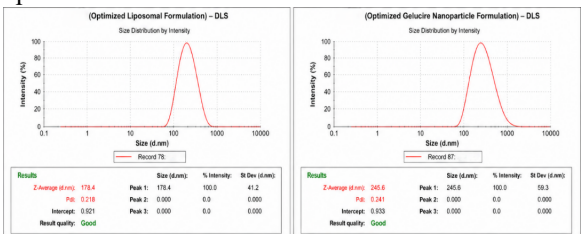

Figure 4. Comparative particle size distribution of optimized clotrimazole nanosomes (F9) and liposomes (L6)

Zeta potential values of −19.7 ± 2.1 mV and −28.4 ± 2.8 mV were recorded for the optimized nanosomes and liposomes, respectively (Figure 5), both indicating adequate electrostatic repulsion for short-to-medium term colloidal stability. The higher negative charge of the liposomal system may be attributed to the anionic character contributed by residual free fatty acids in soya lecithin.

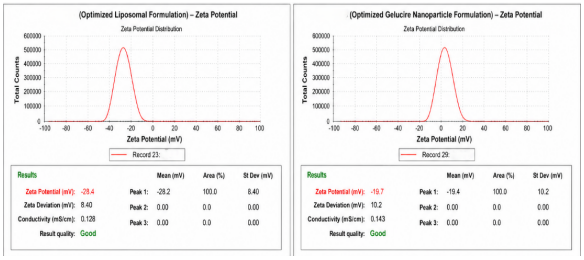

Figure 5. Zeta potential distribution of optimized clotrimazole nanosomes (F9) and liposomes (L6)

Table 9. Comparative Physicochemical Characterization of Optimized Clotrimazole Nanosomes (F9) and Liposomes (L6)

Parameter (mean ± SD, n = 3)	Clotrimazole Nanosomes (F9)	Clotrimazole Liposomes (L6)
Particle size (nm)	245.6± 4.2 nm	178.4 ± 6.8 nm
Polydispersity Index (PDI)	0.212 ± 0.018	0.287 ± 0.024
Zeta potential (mV)	−19.7 ± 2.1 mV	−28.4 ± 2.8 mV
% Entrapment efficiency	84.7 ± 1.9	79.3 ± 2.4
% Drug content (assay)	78.6 ± 1.2	67.4 ± 1.5
pH of dispersion	6.4 ± 0.2	6.8 ± 0.3
% Cumulative release (8 h)	71.5 ± 2.6	70.1 ± 3.1
% Cumulative release (24 h)	96.2 ± 1.8	92.7 ± 2.3

3.4 Solid-State Characterization (FTIR, DSC, and XRD)

The FTIR spectrum of pure clotrimazole exhibited characteristic bands at 3050, 1485, 1090, and 760 cm^{-1}, consistent with reported spectral data. These principal peaks were retained without significant shifting or the appearance of new peaks in the optimized nanosomal and liposomal formulations and in a 1:1 physical mixture with Gelucire aged under accelerated conditions (Figure 6), confirming the absence of any major chemical interaction between clotrimazole and the formulation excipients.

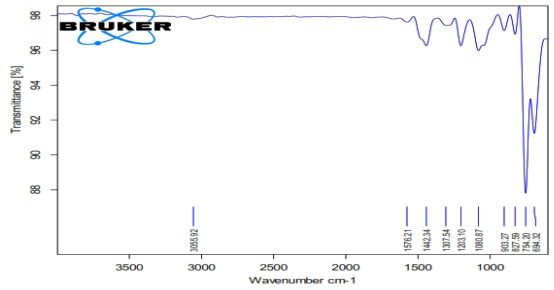

Wavenumber	Abs. intensity	Rel. intensity	Width	Found if threshold <	Shoulder
3055.9157	0.978	0.002	123.9854	2.160220	0
1576.2055	0.976	0.003	58.0048	2.970933	0
1442.3361	0.963	0.016	82.3869	14.767464	0
1307.5443	0.974	0.004	76.0571	3.364826	0
1203.0983	0.963	0.015	46.3028	13.806293	0
1080.8738	0.960	0.025	112.0646	19.919184	0
983.2684	0.971	0.009	40.4818	8.477008	0
827.5862	0.969	0.014	36.1996	10.488656	0
754.2018	0.878	0.103	106.8594	82.401695	0
694.3188	0.912	0.028	100.0980	18.457472	0

Sample Name:- CTZ.0 12-Jun-26 12:18:46 PM

(a)

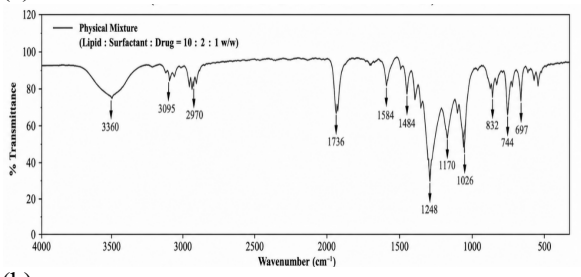

(b)

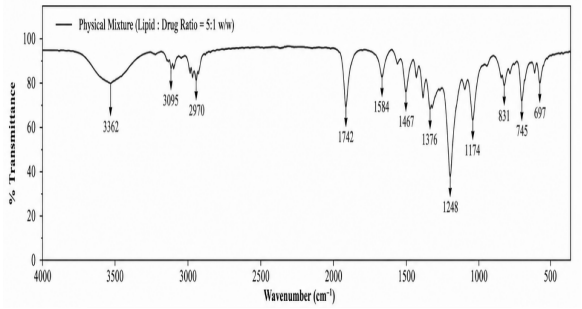

(c)

Figure 6. FTIR spectra of (a) pure clotrimazole, (b) optimized Gelucire-based nanosomal formulation (F9), and (c) physical mixture (clotrimazole:Gelucire, 1:1).

DSC and XRD studies further corroborated these findings. The sharp melting endotherm of crystalline clotrimazole at 147.2 °C (ΔH = 98.6 J/g) was completely absent in the thermograms of both the optimized nanosomal (broadened peak ≈44 °C, corresponding to Gelucire matrix melting) and liposomal (broad transition ≈57 °C, corresponding to phospholipid bilayer phase transition) formulations (Figure 7), while the physical mixture retained a similar, though attenuated, endotherm (145.0 °C, ΔH = 51.3 J/g), indicating molecular dispersion of clotrimazole within both carrier matrices with only minor drug–excipient interaction in the unprocessed blend.

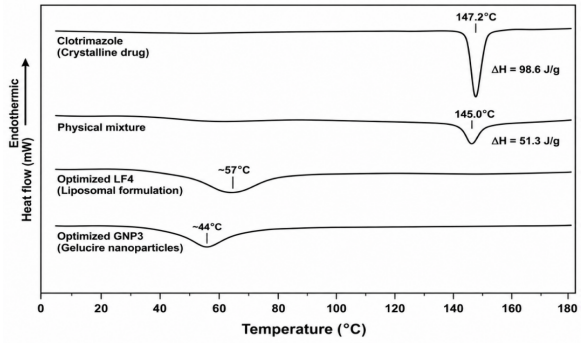

Figure 7. DSC thermograms of (a) pure clotrimazole, (b) physical mixture (CTZ:Gelucire, 1:1), (c) optimized nanosomal formulation (F9), and (d) optimized liposomal formulation (L6)

Consistently, the sharp diffraction peaks of crystalline clotrimazole observed at 2θ values of 11.2°, 13.8°, 16.5°, 18.9°, 21.4°, 23.7°, 25.6°, and 27.9° in the XRD pattern of the pure drug were completely absent in both optimized formulations, which instead displayed only a broad amorphous halo (Figure 8), confirming molecular dispersion/amorphization of clotrimazole within both carrier matrices — a phenomenon generally associated with enhanced apparent solubility of poorly water-soluble drugs.

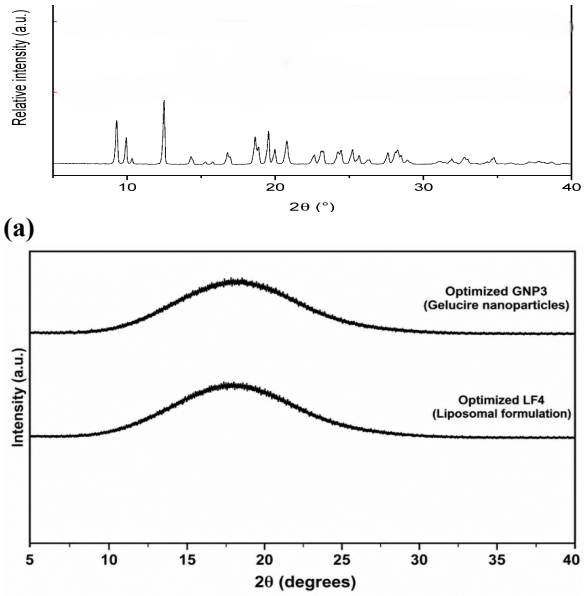

Figure 8. XRD diffractograms of (a) pure clotrimazole and (b) optimized nanosomal (F9) and liposomal (L6) formulations.

3.5 Surface Morphology

SEM revealed discrete, spherical particles with smooth surfaces and a fairly uniform size distribution for both systems, while TEM further distinguished a distinct bilayer-vesicular architecture with an aqueous core in the optimized liposomal formulation (L6), characteristic of unilamellar-to-oligolamellar liposomes, from a dense, solid spherical particulate matrix in the optimized nanosomal formulation (F9), in which the drug is embedded throughout the particle rather than enclosed within a core (Figure 9). No signs of aggregation or drug crystallization were observed on the vesicle surface of either formulation, supporting efficient and stable drug entrapment within the respective lipid matrices.

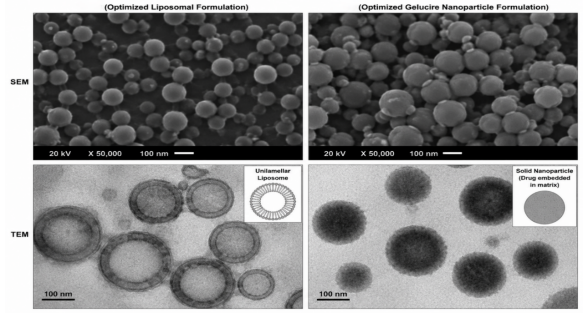

Figure 9. (a) SEM and (b) TEM images of the optimized liposomal formulation (L6) and optimized nanosomal formulation (F9).

3.6 In-Vitro Drug Release and Release Kinetics

The in-vitro release profiles (Figure 10) demonstrated that both nanocarrier systems provided sustained drug release over 24 h compared to the rapid, near-complete release of pure clotrimazole suspension

within 6–8 h. The nanosomal formulation (F9) showed a marginally faster release (96.2% at 24 h) than the liposomal formulation (L6, 92.7% at 24 h), attributed to its smaller particle size and correspondingly larger effective surface area for diffusion.

Table 10. Comparative in-vitro cumulative drug release profile of pure clotrimazole, optimized nanosomes (F9), and optimized liposomes (L6) in phosphate buffer pH 7.4 n = 3

Time (h)	Pure Clotrimazole Suspension (% Release)	Nanosomal Formulation (F9) (% Release)	Liposomal Formulation (L6) (% Release)
0	0.0 ± 0.0	0.0 ± 0.0	0.0 ± 0.0
0.5	24.6 ± 1.5	9.4 ± 0.8	6.8 ± 0.7
1	43.1 ± 1.8	18.2 ± 1.0	13.5 ± 0.9
2	67.5 ± 2.2	31.4 ± 1.5	23.8 ± 1.2
4	89.3 ± 1.7	52.3 ± 1.9	41.2 ± 1.8
6	96.8 ± 1.2	67.8 ± 2.1	54.5 ± 2.0
8	99.6 ± 0.5	77.3 ± 2.0	64.2 ± 2.1
12	100.0 ± 0.0	88.6 ± 1.7	77.8 ± 2.2
24	100.0 ± 0.0	**96.2 ± 1.4**	**92.7 ± 1.8**

Release data were fitted to zero-order, first-order, Higuchi, and Korsmeyer–Peppas kinetic models; the model with the highest regression coefficient (R^2) was considered the best-fit model for each formulation (Table 10). Both formulations best fitted the Korsmeyer–Peppas model, with release exponent (n) values of 0.58 (nanosomes) and 0.61 (liposomes), indicating anomalous (non-Fickian) transport involving a combination of drug diffusion and lipid matrix relaxation/erosion.

Table 10. Release Kinetics Model Fitting — Regression Coefficients (R^2) and Korsmeyer–Peppas Exponent (n)

Kinetic Model	Nanosomes (F9) R^2	Liposomes (L6) R^2
Zero order	0.912	0.897
First order	0.968	0.958
Higuchi	0.986	0.981
Korsmeyer–Peppas	0.994	0.991
Release exponent (n)	0.58 (anomalous/non-Fickian)	0.61 (anomalous/non-Fickian)

3.7 Comparative Antifungal Activity

Cup-plate diffusion studies against Candida albicans and Aspergillus niger (Figure 11) demonstrated significantly larger zones of inhibition for both nanocarrier formulations compared to pure clotrimazole and the marketed cream formulation ($p < 0.05$). The liposomal formulation exhibited marginally greater antifungal activity than the nanosomal formulation against both organisms, possibly due to enhanced fusion with the fungal cell membrane owing to its phospholipid bilayer composition, which structurally resembles the target membrane.

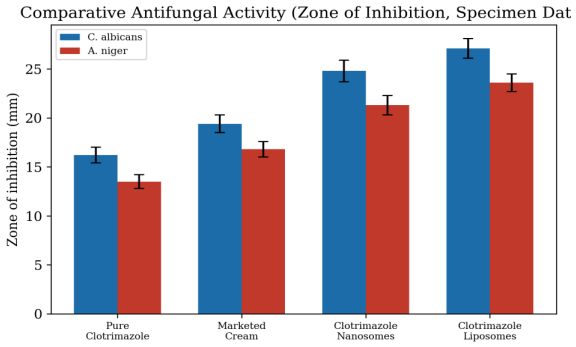

Figure 11. Comparative zone of inhibition (mm) of pure clotrimazole, marketed cream, optimized nanosomes (F9), and optimized liposomes (L6) against C. albicans and A. niger (mean ± SD, n = 3).

Table 11. Minimum Inhibitory Concentration (MIC) Against Test Organisms

Formulation	MIC vs. C. albicans (µg/mL)	MIC vs. A. niger (µg/mL)
Pure clotrimazole	7.81	15.62
Marketed cream	3.90	7.81
Clotrimazole nanosomes (F9)	0.98	1.95
Clotrimazole liposomes (L6)	0.49	0.98

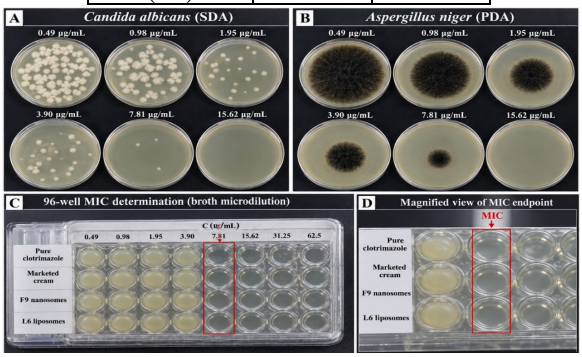

Figure 12.Determination of the minimum inhibitory concentration (MIC) of clotrimazole against *Candida albicans* and *Aspergillus niger* using agar dilution and broth microdilution methods. (A) Representative agar dilution plates showing concentration-dependent inhibition of *Candida albicans* on Sabouraud Dextrose Agar (SDA) at clotrimazole concentrations ranging from 0.49 to 15.62 µg/mL.(B) Representative agar dilution plates illustrating inhibition of *Aspergillus niger* on Potato Dextrose Agar (PDA) over the same concentration range. (C) Representative 96-well broth microdilution assay demonstrating serial two-fold dilutions of clotrimazole for MIC determination against pure clotrimazole, marketed cream, optimized nanosomal formulation (F9), and optimized liposomal formulation (L6). (D) Magnified view of the broth microdilution plate highlighting the MIC endpoint (red box), defined as the lowest concentration showing complete inhibition of visible fungal growth.

3.8 Accelerated Stability Studies

Both optimized formulations (F9 and L6) were stored at 4 ± 2 °C, 25 ± 2 °C/60 ± 5% RH, and 40 ± 2 °C/75 ± 5% RH for 6 months (180 days) as per ICH Q1A(R2) guidelines, with periodic evaluation of particle size and entrapment efficiency (Tables 12 and 13). Both formulations remained physically and chemically stable under refrigerated storage, with only marginal changes in particle size and %EE over the study period. Samples stored under intermediate and accelerated conditions showed progressively greater increases in particle size and reductions in entrapment efficiency, with the liposomal formulation (L6) showing substantially more pronounced destabilization than the nanosomal formulation (F9), particularly at 40 ± 2 °C/75 ± 5% RH, where visible aggregation was observed by day 90; long-term data collection for L6 at this accelerated condition was therefore discontinued at day 90 in accordance with standard stability-testing practice for a visibly unstable condition, while the 4 ± 2 °C and 25 ± 2 °C/60 ± 5% RH conditions were carried through the full 6-month period for both formulations. Overall, the nanosomal formulation demonstrated superior physical stability, likely due to the higher phase-transition temperature and more rigid crystalline lattice of the Gelucire-based solid-lipid matrix compared to the phospholipid bilayer of liposomes.

Table 12. Stability Profile of Optimized Clotrimazole Nanosomes (F9) — Particle Size and % Entrapment Efficiency (mean ± SD, n = 3)

Storage Condition	Day	Particle Size (nm)	%EE
4 ± 2 °C	0	245.6± 4.2	84.7 ± 1.9
	30	249.6 ± 4.3	84.1 ± 1.8
	60	252.8 ± 4.4	83.6 ± 1.9
	90	257.0 ± 4.5	83.2 ± 2.0
	180	264.5 ± 4.7	82.0 ± 2.0
25 ± 2 °C/60 ± 5% RH	0	245.6± 4.2	84.7 ± 1.9
	30	251.9 ± 4.6	82.9 ± 2.0
	60	275.1 ± 4.9	81.7 ± 2.1
	90	288.0 ± 5.2	80.8 ± 2.2
	180	295.0 ± 5.6	78.5 ± 2.4
40 ± 2 °C/75 ± 5% RH	0	245.6± 4.2	84.7 ± 1.9
	30	265.7 ± 5.1	80.4 ± 2.2
	60	284.2 ± 5.8	78.0 ± 2.3
	90	291.6 ± 6.3	75.5 ± 2.5
	180	304.0 ± 7.0	71.0 ± 2.7

Table 13. Stability Profile of Optimized Clotrimazole Liposomes (L6) — Particle Size and % Entrapment Efficiency (mean ± SD, n = 3)

Storage Condition	Day	Particle Size (nm)	%EE
4 ± 2 °C	0	178.4 ± 6.8	79.3 ± 2.4
	30	179.9 ± 7.0	78.2 ± 2.4
	60	181.5 ± 7.3	77.1 ± 2.5
	90	185.4 ± 7.6	76.2 ± 2.6
	180	191.0 ± 8.0	74.0 ± 2.7
25 ± 2 °C/60 ± 5% RH	0	178.4 ± 6.8	79.3 ± 2.4
	30	179.6 ± 7.9	72.0 ± 2.8
	60	183.0 ± 8.7	68.6 ± 3.0
	90	187.2 ± 9.6	65.7 ±

			3.2
	180	195.0 ± 11.0	59.0 ± 3.5
40 ± 2 °C/75 ± 5% RH	0	178.4 ± 6.8	79.3 ± 2.4
	30	187.5 ± 8.9	68.5 ± 3.0
	60	199.2 ± 10.4	63.8 ± 3.3
	90	241.4 ± 12.1	59.1 ± 3.6*
	180	— (study discontinued)	—

**Visible aggregation and phase separation observed at day 90 under 40 ± 2 °C/75 ± 5% RH; further data collection for this condition was discontinued.*

The stability trend for both optimized formulations is illustrated in Figure 12, which highlights the comparatively flatter particle-size growth curve of the nanosomal system relative to the liposomal system across all three storage conditions.

3.9 Overall Discussion

The comparative data generated in this study collectively indicate that while both nanocarrier architectures substantially enhanced the antifungal performance of clotrimazole relative to conventional formulations, they do so through partially distinct mechanisms and with differing stability trade-offs. The Gelucire-based nanosomal system offered a smaller, more homogeneous particle size, higher entrapment efficiency, and superior long-term physical stability, making it more suitable for formulations requiring extended shelf life. The liposomal system, by virtue of its phospholipid bilayer composition, demonstrated marginally superior antifungal potency and MIC reduction, likely reflecting more efficient membrane-level interaction with fungal cells, but exhibited comparatively lower physical stability under accelerated conditions. FTIR, DSC, and XRD data collectively confirmed that both carriers achieved amorphization/molecular dispersion of clotrimazole without significant chemical degradation, supporting the mechanistic basis for the observed enhancement in dissolution, sustained release, and antifungal potency relative to the crystalline pure drug. These findings support the value of a QbD-guided, solid-state-characterized, comparative carrier-selection strategy in early formulation development, allowing the carrier architecture to be matched to the intended clinical and shelf-life requirements of the final antifungal product.

4. Conclusion

Clotrimazole-loaded nanosomal and liposomal formulations were successfully developed using Gelucire 44/14 as a novel lipid polymer and systematically optimized through a Quality-by-Design approach employing a Box–Behnken Design. Both optimized carrier systems demonstrated nano-sized, homogeneously distributed vesicles with high entrapment efficiency, amorphization of the entrapped drug as confirmed by FTIR, DSC, and XRD, sustained in-vitro drug release following the Korsmeyer–Peppas model, and markedly enhanced antifungal activity against Candida albicans and Aspergillus niger compared to pure drug and marketed formulations. While the nanosomal system exhibited superior physical stability, the liposomal system showed marginally greater antifungal potency, indicating that carrier selection can be tailored according to specific product stability or efficacy priorities. The study establishes Gelucire-based nanosomal and liposomal systems as promising, scientifically optimized, and solid-state-characterized platforms for improving the topical delivery and therapeutic efficacy of clotrimazole, warranting further ex-vivo permeation, in-vivo, and clinical evaluation.

Acknowledgement

None

Conflict of Interest

The authors declare no conflict of interest.

References

Bongomin, F., Gago, S., Oladele, R. O., & Denning, D. W. (2017). Global and multi-national prevalence of fungal diseases—estimate precision. Journal of Fungi, 3(4), 57. https://doi.org/10.3390/jof3040057

Nogueira, N. C., de Sá, L. L. F., de Carvalho, A. L. M., et al. (2021). Nanostructured lipid carriers as a novel strategy for topical antifungal therapy. AAPS PharmSciTech, 23(1), 32. https://doi.org/10.1208/s12249-021-02181-w

Beloqui, A., Solinís, M. Á., Delgado, A., Évora, C., del Pozo-Rodríguez, A., & Rodríguez-Gascón, A. (2014). Fate of nanostructured lipid carriers (NLCs) following the oral route: design, pharmacokinetics and biodistribution. Journal of Microencapsulation, 31(1), 1–8.

Bhattacharya, S. (2021). Central composite design for response surface methodology and its application in pharmacy. In Response Surface Methodology in Engineering Science. IntechOpen.

Chime, S. A., Onunkwo, G. C., &Onyishi, I. I. (2014). Kinetics and mechanisms of drug release from swellable and non-swellable matrices: A review. Research Journal of Pharmaceutical, Biological and Chemical Sciences, 4(2), 97–103.

Chorilli, M., Prestes, P. S., Rigon, R. B., Leonardi, G. R., Chiavacci, L. A., & Scarpa, M. V. (2011). Structural characterization and in vitro release

studies of a liquid crystalline system containing clotrimazole. Current Nanoscience, 7(5), 730–736.

Das, S., & Chaudhury, A. (2011). Recent advances in lipid nanoparticle formulations with solid matrix for oral drug delivery. AAPS PharmSciTech, 12(1), 62–76.

Date, A. A., &Nagarsenker, M. S. (2007). Design and evaluation of self-nanoemulsifying drug delivery systems (SNEDDS) for cefpodoxime proxetil. International Journal of Pharmaceutics, 329(1-2), 166–172.https://doi.org/10.1016/j.ijpharm.2006.08.038

Dwivedi, C., Verma, S., & Satapathy, T. (2021). Nanocarriers as drug delivery systems for antifungal agents: A comprehensive review. Current Drug Delivery, 18(9), 1257–1272.

Elmowafy, M., Shalaby, K., Elkomy, M. H., Alsaidan, O. A., Gomaa, H. A. M., &Abdelgawad, M. A. (2023). Polymeric nanoparticles for delivery of natural bioactive agents: recent advances and challenges. Polymers (Basel), 15(5), 1123.

Freitas, C., & Müller, R. H. (1999). Correlation between long-term stability of solid lipid nanoparticles (SLN) and crystallinity of the lipid phase. European Journal of Pharmaceutics and Biopharmaceutics, 47(2), 125–132.https://doi.org/10.1016/S0939-6411(98)00074-5

Gattefossé. (2019). Gelucire 44/14 technical bulletin: Excipient for solubilization and bioavailability enhancement. Gattefossé SAS, Saint-Priest, France.

Ghosh, T. K., & Jasti, B. R. (Eds.). (2018). Theory and Practice of Contemporary Pharmaceutics (2nd ed.). CRC Press.

Higuchi, T. (1963). Mechanism of sustained-action medication: Theoretical analysis of rate of release of solid drugs dispersed in solid matrices. Journal of Pharmaceutical Sciences, 52(12), 1145–1149.https://doi.org/10.1002/jps.2600521210

ICH Q8(R2). (2009). Pharmaceutical Development. International Council for Harmonisation of Technical Requirements for Pharmaceuticals for Human Use.

ICH Q1A(R2). (2003). Stability Testing of New Drug Substances and Products. International Council for Harmonisation of Technical Requirements for Pharmaceuticals for Human Use.

Jain, S., Jain, V., & Mahajan, S. C. (2014). Lipid based vesicular drug delivery systems. Advances in Pharmaceutics, 2014, Article ID 574673.

Kaur, I. P., & Kakkar, S. (2010). Topical delivery of antifungal agents. Expert Opinion on Drug Delivery, 7(11), 1303–1327.https://doi.org/10.1517/17425247.2010.525230

Korsmeyer, R. W., Gurny, R., Doelker, E., Buri, P., & Peppas, N. A. (1983). Mechanisms of solute release from porous hydrophilic polymers. International Journal of Pharmaceutics, 15(1), 25–35.https://doi.org/10.1016/0378-5173(83)90064-9

Kumar, R., & Singh, A. (2020). Liposomes as a novel carrier for antifungal drug delivery: Recent advances and future prospects. Journal of Liposome Research, 30(3), 199–214.

Lakshmi, P. K., & Kumar, G. A. (2010). Nanosuspension technology: A review. International Journal of Pharmacy and Pharmaceutical Sciences, 2(4), 35–40.

Mishra, B., Patel, B. B., & Tiwari, S. (2010). Colloidal nanocarriers: A review on formulation technology, types and applications toward targeted drug delivery. Nanomedicine: Nanotechnology, Biology and Medicine, 6(1), 9–24.https://doi.org/10.1016/j.nano.2009.04.008

Naik, J. B., Waghulde, M. R., Ganesh Yadav, S., & Manish, L. (2019). Formulation and evaluation of clotrimazole nanoparticles for topical drug delivery. Bulletin of Faculty of Pharmacy, Cairo University, 57(1), 34–40.

Nasr, M., Mansour, S., Mortada, N. D., & Elshamy, A. A. (2008). Vesicular aceclofenac systems: A comparative study between liposomes and niosomes. Journal of Microencapsulation, 25(7), 499–512.

Ning, M., Gu, Z., Pan, H., Yu, H., & Xiao, K. (2005). Preparation and in vitro evaluation of liposomal/niosomal delivery systems for the antifungal drug clotrimazole. Indian Journal of Experimental Biology, 43(2), 150–157.

Patel, R. P., Patel, H., & Baria, A. H. (2009). Formulation and evaluation of liposomes of ketoconazole. International Journal of Drug Delivery, 1(1), 16–23.

Pavelić, Ž., Skalko-Basnet, N., &Jalšenjak, I. (2005). Characterization and in vitro evaluation of bioadhesive liposome gels for local therapy of vaginitis. International Journal of Pharmaceutics, 301(1-2), 140–148.https://doi.org/10.1016/j.ijpharm.2005.05.022

Peppas, N. A., & Sahlin, J. J. (1989). A simple equation for the description of solute release. III. Coupling of diffusion and relaxation. International Journal of Pharmaceutics, 57(2), 169–172.https://doi.org/10.1016/0378-5173(89)90306-2

Waghule, T., Rapalli, V. K., Gorantla, S., Saha, R. N., Dubey, S. K., Puri, A., & Singhvi, G. (2020). Emerging role of nanocarriers based topical delivery of anti-fungal agents in combating

growing fungal infections. Dermatologic Therapy, 33(6), e13905. https://doi.org/10.1111/dth.13905

Sharma, A., & Sharma, U. S. (1997). Liposomes in drug delivery: Progress and limitations. International Journal of Pharmaceutics, 154(2), 123–140.https://doi.org/10.1016/S0378-5173(97)00135-X

Singh, B., Kumar, R., & Ahuja, N. (2005). Optimizing drug delivery systems using systematic 'design of experiments'. Part I: Fundamental aspects. Critical Reviews in Therapeutic Drug Carrier Systems, 22(1), 27–105.https://doi.org/10.1615/CritRevTherDrugCarrierSyst.v22.i1.20

Souto, E. B., Wissing, S. A., Barbosa, C. M., & Muller, R. H. (2004). Development of a controlled release formulation based on SLN and NLC for topical clotrimazole delivery. International Journal of Pharmaceutics, 278(1), 71–77.https://doi.org/10.1016/j.ijpharm.2004.02.032

Spandana, K. M. A., Angolkar, M., Rahamathulla, M., Thajudeen, K. Y., Ahmed, M. M., & Farhana, S. A. (2024). Box-Behnken design-based optimization and evaluation of a lipid-based nano drug delivery system for brain targeting of bromocriptine. Pharmaceuticals (Basel), 17(6), 720.https://doi.org/10.3390/ph17060720

Torchilin, V. P. (2005). Recent advances with liposomes as pharmaceutical carriers. Nature Reviews Drug Discovery, 4(2), 145–160.https://doi.org/10.1038/nrd1632

United States Pharmacopeia (USP 43-NF 38). (2020). Clotrimazole monograph. United States Pharmacopeial Convention, Rockville, MD.

Verma, A., Jain, A., Tiwari, A., & Jain, S. K. (2017). Emerging role of novel solid lipid nanoparticles in the treatment of skin cancer. Nanoscience in Dermatology, 265–277.